Role of the circular RNA regulatory network in the pathogenesis of biliary atresia

DONG LIU[1], YINGHUI DONG[2], JIAHUI GAO[1], ZHOUGUANG WU[1], LIHUI ZHANG[3] and BIN WANG[1]

[1]Department of General Surgery, Shenzhen Children's Hospital; [2]Department of Ultrasound, Shenzhen People's Hospital; [3]Department of Traditional Chinese Medicine, Shenzhen Children's Hospital, Shenzhen, Guangdong 518000, P.R. China

Received March 24, 2023; Accepted November 13, 2023

DOI: 10.3892/etm.2024.12383

Abstract. Circular RNAs (circRNAs) serve an essential role in the occurrence and development of cholangiocarcinoma, but the expression and function of circRNA in biliary atresia (BA) is not clear. In the present study, circRNA expression profiles were investigated in the liver tissues of patients with BA as well as in the choledochal cyst (CC) tissues of control patients using RNA sequencing. A total of 78 differentially expressed circRNAs (DECs) were identified between the BA and CC tissues. The expression levels of eight circRNAs (hsa_circ_0006137, hsa_circ_0079422, hsa_circ_0007375, hsa_circ_0005597, hsa_circ_0006961, hsa_circ_0081171, hsa_circ_0084665 and hsa_circ_0075828) in the liver tissues of the BA group and control group were measured using reverse transcription-quantitative polymerase chain reaction. Gene Ontology (GO) and Kyoto Encyclopedia of Genes and Genomes (KEGG) pathway enrichment analysis demonstrated that the identified DECs are involved in a variety of biological processes, including apoptosis and metabolism. In addition, based on the GO and KEGG pathway enrichment analyses, it was revealed that target genes that can be affected by circRNAs regulatory network were enriched in the TGF-β signaling pathway, EGFR tyrosine kinase inhibitor resistance pathway and transcription factor regulation pathway as well as other pathways that may be associated with the pathogenesis of BA. The present study revealed that circRNAs are potentially implicated in the pathogenesis of BA and could help to find promising targets and biomarkers for BA.

Correspondence to: Dr Lihui Zhang, Department of Traditional Chinese Medicine, Shenzhen Children's Hospital, 7019 Yitian Road, Futian, Shenzhen, Guangdong 518000, P.R. China
E-mail: wqq1225@yeah.net

Dr Bin Wang, Department of General Surgery, Shenzhen Children's Hospital, 7019 Yitian Road, Futian, Shenzhen, Guangdong 518000, P.R. China
E-mail: szwb1967@hotmail.com

Key words: RNA sequencing, circular RNA, biliary atresia, regulatory network, functional prediction

Introduction

Biliary atresia (BA) is a rare destructive inflammatory disease that occurs in infancy and affects the intrahepatic and extrahepatic bile duct system to varying degrees, resulting in intrahepatic cholestasis, intrahepatic and extrahepatic bile duct obstruction, progressive liver fibrosis and malignant progression to liver cirrhosis (1,2). It has a high incidence in Asia, occurring in ~1:5,000 live births (3), while in Western countries the incidence is relatively low, ~1:15,000-19,000 live births (4). According to the clinical manifestations, BA can be divided into perinatal and fetal types. The perinatal type accounts for ~90% and the majority of patients have no concomitant malformations. The fetal type accounts for ~10% with jaundice occurring in the early postnatal period, and the majority of patients are also accompanied by congenital malformations, such as BA and splenic malformation syndrome (5). BA can also be divided into three types according to the level of proximal biliary obstruction. In type I BA (accounting for 5%), atresia occurs at the common bile duct, and there is often a cyst structure in the proximal end of the atresia. In type II BA (accounting for 2%), obstruction occurs at the common hepatic duct. In type III BA (accounting for >90%), the extrahepatic bile duct is completely atretic, and the hepatic hilum is a fibrotic solid structure (6). At present, the etiology of BA is not clear, and it is considered to be the final result of multiple conditions, such as sclerosing occlusive inflammatory biliary disease. Possible causes include congenital genetic factors, infection factors accompanied by inflammation and immune response, maternal factors and vascular factors (7-9). Therefore, studying the molecular mechanism of BA is a key scientific issue in the clinic that needs to be solved.

Circular RNA (circRNA) is a type of non-coding RNA molecule that does not have a 5'-terminal cap or a 3'-terminal poly (A) tail and forms a ring structure with covalent bonds. As circRNA molecules have a closed ring structure, they are not affected by RNA exonucleases in cells, they are not easy to degrade and their expression is more stable (10,11). Previous studies (12-14) have shown that circRNA molecules contain binding sites for microRNA (miRNA/miR) or RNA binding proteins, which act as miRNA sponges and trans-acting factors in cells, suggesting that circRNA may influence and regulate human diseases by regulating disease-associated miRNAs (15). Furthermore, a number of previous studies

have shown that circRNAs are associated with numerous diseases, such as systemic lupus erythematosus (16), coronary artery disease (17), several types of cancer (such as breast and stomach cancer) (18) and nervous system disease (19). However, there have been only a small number of studies on the circRNA regulatory network in BA, and the mechanism of most circRNAs in BA is still in its infancy. With the development of next-generation sequencing and bioinformatics analysis, circRNA research is progressing. Numerous circRNAs are demonstrated to be involved in the progression of a number of diseases, and because of their conservation, stability, specificity, richness and easy detection (20) they not only point out a new direction for clinical treatment, but also provide new markers for the early diagnosis of BA. A number of circRNAs also provide novel ideas for clarifying the mechanism of the circRNA-miRNA axis in the process of liver fibrosis (21,22).

In the present study, DECs between BA and CC tissues were identified based on high-throughput RNA sequencing. Subsequently, eight candidate circRNAs were selected and their expression levels in the liver tissues of patients with BA and control patients with choledochal cyst (CC) were detected using reverse transcription-quantitative polymerase chain reaction (RT-qPCR). The miRNAs that can bind to the eight circRNAs and their downstream target genes were predicted using bioinformatics technology, and Gene Ontology (GO) and Kyoto Encyclopedia of Genes and Genomes (KEGG) pathway enrichment analysis were carried out. The results of the present study provided an important theoretical basis for the molecular mechanism of the circRNA network in regulating the occurrence and development of BA.

Materials and methods

Sample preparation. Between April 2018 and May 2020, 38 patients with BA and 54 patients with choledochal cysts (CCs) were enrolled in the present study. All patients were diagnosed via laparoscopic bile duct exploration by the same surgical team at Shenzhen Children's Hospital (Shenzhen, China), and liver biopsy tissues were obtained at the time of surgery. The mean age of the patients in the BA group was 72.58±27.31 days, and the group included 15 male and 23 female patients (Table SII). The mean age of the patients in the CC group was 40.32±38.62 months, and the group included 14 male and 40 female patients (Table SIII). The liver tissues were immersed in RNA sample preservation solution (cat. no. R916331; Macklin, Inc.) and cryopreserved at -80˚C. The patients did not receive any treatment before surgery. The present study was approved by the Ethics Committee of Shenzhen Children's Hospital (approval no. SUMC2017-026). The parents of all the subjects provided written informed consent.

RNA isolation. TRIzol® reagent (Invitrogen; Thermo fisher Scientific, Inc.) was used to extract total RNA from BA liver tissues as well as CC tissues. The concentration and purity of RNA was detected using a Nanodrop-1000 (Thermo Fisher Scientific, Inc.) and Qubit RNA HS Assay Kit (cat. no. Q32852; Thermo Fisher Scientific, Inc.), then the yield and quality was evaluated using an Agilent 2100 Bioanalyzer (Agilent Technologies, Inc.) to test the integrity of the RNA. All RNA integrity numbers were >7 to ensure RNA quality.

Library construction and sequencing. Before the construction of the library, ribosomal RNA (rRNA) was removed using a Ribo-Zero Plus rRNA Depletion Kit (cat. no. 20037135; Illumina, Inc.). NEBNext® Multiplex Small RNA Library Prep Set (cat. no. E7330S; Illumina, Inc.) was used to generate a sequencing library. To map the sequence to each sample, a barcode had to be added. Subsequently, the quality of the library was examined using a RNA high sensitivity chip on an Agilent 2100 Bioanalyzer (Agilent Technologies, Inc.). VAHTS Library Quantification Kit for Illumina (cat. no. NQ101; Vazyme, Inc.) was used to accurately quantify the effective concentration of the library with an ABI StepOnePlus Real-Time PCR system (cat. no. 4376600; Applied Biosystems; Thermo Fisher Scientific, Inc.). The library was diluted to 20 pM as the final concentration. Then a sample cluster was performed on the cBot cluster generation system (cat. no. SY-312-2001; Illumina, Inc.) with TruSeq PE Cluster kit v3-cBot-HS (cat. no. 20015963; Illumina, Inc.), followed by paired-end sequencing of 125-bp reads with the Illumina HiSeq 2500 platform (Illumina, Inc.). All steps followed the manufacturer's protocols.

Sequencing data analysis and circRNA analysis. The accuracy of the sequencing results of the extracted RNA from liver BA and CC tissues was verified by filtering the sequencing data. Using Trimmomatic (23), the reads containing adapters were removed, then the low-quality sequences at the 5' and 3' ends were trimmed, and the reads containing >5% N bases were removed. This produced high-quality clean reads for all downstream analyses. The reference genome as well as gene annotation files were downloaded from the Ensembl genome browser (Ensembl GRCh37 release 110-July 2023; https://grch37.ensembl.org/index.html). The sequencing reads were mapped to the human genome using the HISAT2 software, and circRNAs were identified using 'circRNA_finder' analysis. Additionally, the expression of known miRNAs was compared with the precursor and mature miRNA sequences in miRbase (version 22) (24) using default parameters (25). The differentially expressed mRNAs, miRNAs and circRNAs were identified using the edgeR software package (26), with P<0.05 and log2 fold-change (FC)>1 as selection parameters. The pheatmap R package (https://cran.r-project.org/web/packages/pheatmap/pheatmap.pdf) was used to cluster the samples. CircRNA sequencing was performed by Vazyme Biotech Co., Ltd. qPCR was performed to verify the expression of circRNA in tissue samples and all primer sequences are presented in Table SI.

Functional and pathway enrichment analysis. R software (version 4.0.2; https://cran.r-project.org/doc/contrib/Liu-R-refcard.pdf) was used to estimate DECs between BA and CC samples. GO (https://geneontology.org/) term enrichment analysis was performed, including molecular function, cellular component and biological process, along with KEGG (http://www.genome.ad.jp/kegg/) analysis. DECs were identified using the clusterProfiler (http://www.bioconductor.org/

packages/release/bioc/html/clusterProfiler.html), org.Hs.eg.db (http://www.bioconductor.org/packages/release/data/annotation/html/org.Hs.eg.db.html), enrichplot (http://www.bioconductor.org/packages/release/bioc/html/enrichplot.html) and ggplot2 packages (https://cran.rstudio.com/bin/windows/contrib/4.2/ggplot2_3.4.2.zip) in Bioconductor, which is an R package used to perform GO functional and KEGG pathway enrichment analysis.

RT-qPCR. The expression of the circRNAs was validated using BA and CC tissues. Liver tissues were frozen in liquid nitrogen and then crushed into a homogenate. Total RNA was extracted using TRIzol® reagent and transcribed into cDNA using an rtSTAR™ First-Strand cDNA synthesis kit (cat. no. AS-FS-003-02; Arraystar, Inc.). Specific primers (presented in Table SI) were designed with Primer Premier 5.0 (Premier Biosoft), and synthesized by Vazyme Biotech Co., Ltd. Following the manufacturer's protocols, Arraystar SYBR® Green Real-time qPCR Master Mix (Arraystar Inc.) was used for qPCR. The cycling conditions were 5 min at 95˚C for the initial denaturation period, then 15 sec at 95˚C for denaturation and 1 min at 60˚C for annealing and extension, repeated for 40 cycles. Expression levels were normalized to endogenous control (taqman endogenous controls FG, Human GAPDH; cat. no. 4352934E; Applied Biosystem; Thermo Fisher Scientific, Inc.), and the FC relative to circRNA expression levels in the CC group was calculated using the $2^{-\Delta\Delta Cq}$ method according to a previous study (27). All steps followed the manufacturers' protocols.

Target gene prediction and functional enrichment analysis. StarBase (v2.0) (28), TargetScan (https://www.targetscan.org/vert_80/) and miRanda software (https://cbio.mskcc.org/miRNA2003/miranda.html) were used to predict the downstream miRNAs of the circRNAs. The target mRNAs of candidate miRNAs were further analyzed using the miRDB (https://mirdb.org/custom.html), miRTarBase (https://mirtarbase.cuhk.edu.cn) and TargetScan databases. Subsequently, functional enrichment analysis of these mRNAs was carried out as a Venn diagram using R software. All databases were used according to default parameters.

Network visualization. In the present study, the online tool Search Tool for the Retrieval of Interacting Genes/Proteins (https://string-db.org/) was used to analyze the protein-protein interaction (PPI) of the predicted target genes, and Cytoscape software (version 3.4.0) (29,30) was used to construct the PPI network. Through node observation, the key nodes of the PPI network were examined. The Wilcoxon rank sum test was used to test for significant differences in topological properties between the BA and CC groups.

Receiver operating characteristic (ROC) curve analysis. To evaluate the impact of differential gene expression on the disease status of BA, ROC curve analysis was used. This was conducted by plotting the ROC curve using gene expression data juxtaposed with the sample state (with or without BA), thereby enabling an assessment of gene expression accuracy (31). The pROC package in R software was used to generate these ROC curves (31). The entropy weight method was used to determine the entropy weight of each gene, following which the ROC curves for five genes with significant differences between the BA and CC groups were plotted. The accuracy of each biomarker was determined by the area under the curve (AUC) derived from the ROC curve analysis.

Statistical analysis. R software was used to integrate and analyze the data. Continuous variables are expressed as the mean ± standard deviation (at least 3 experimental repeats). An independent samples t-test was used to compare the continuous variables between BC and CC groups, as the samples were independent from each other. The figures were prepared using GraphPad Prism 8.0 (GraphPad Software; Dotmatics). $P<0.05$ was considered to indicate a statistically significant difference.

Results

Identification and annotation of circRNAs. In the present study, the sequencing reads were first mapped to the human genome, and the circRNAs were then systematically identified and annotated using 'circRNA_finder' analysis. In total, 7,349 circRNAs were identified and three types of circRNAs were revealed, including exon, intergenic and intron circRNAs. Among them, most circRNAs (83.4%) were of the exon type, 6.4% were intergenic and 7.9% were intron type (a small percentage were not annotated). circRNA transcripts were distributed in the majority of chromosomes (Chr) (Fig. 1A). circRNAs from Chr1, Chr2, Chr3 and Chr13 accounted for 9.49, 7.48, 6.18 and 5.58%, respectively. These chromosomes corresponded to more than half of the RNAs of interest. In addition, the length of the circRNAs from these four chromosomes ranged from 152-9,637 bp, and the distribution frequency was 69.3% for circRNAs ranging from 152-1,000 bp and 16.4% for circRNAs >2,000 bp (Fig. 1B).

Identification of DECs in BA. To identify the DECs associated with BA and CC, high-throughput analysis was performed on liver tissues from BA and CC cases (3 cases each). The R software package was used to analyze the differential expression, and a list of upregulated and downregulated DECs was obtained. According to the criteria of log2FC >2 and $P<0.05$, there were 78 DECs, including 16 upregulated circRNAs and 62 downregulated circRNAs (Fig. 2A). The top five upregulated genes and the top three downregulated genes (using the volcano map in Fig. 2B) were selected for subsequent RT-qPCR verification. Table I presents the names of all upregulated and downregulated circRNAs.

Functional and pathway enrichment analysis of DECs. GO functional and KEGG pathway enrichment analysis were performed on the host genes of the 78 DECs using R software. The results of GO analysis indicated that the main biological processes of these host genes were 'positive regulation of catabolic process', 'negative regulation of catabolic processes', 'regulation of microtubule motor activity' and 'cellular response to alcohol'. The primary cellular component category consisted of the categories 'intracellular part', 'organelle part', 'plasma membrane region' and 'cytoplasm'. Finally, the main molecular functions included 'enzyme binding',

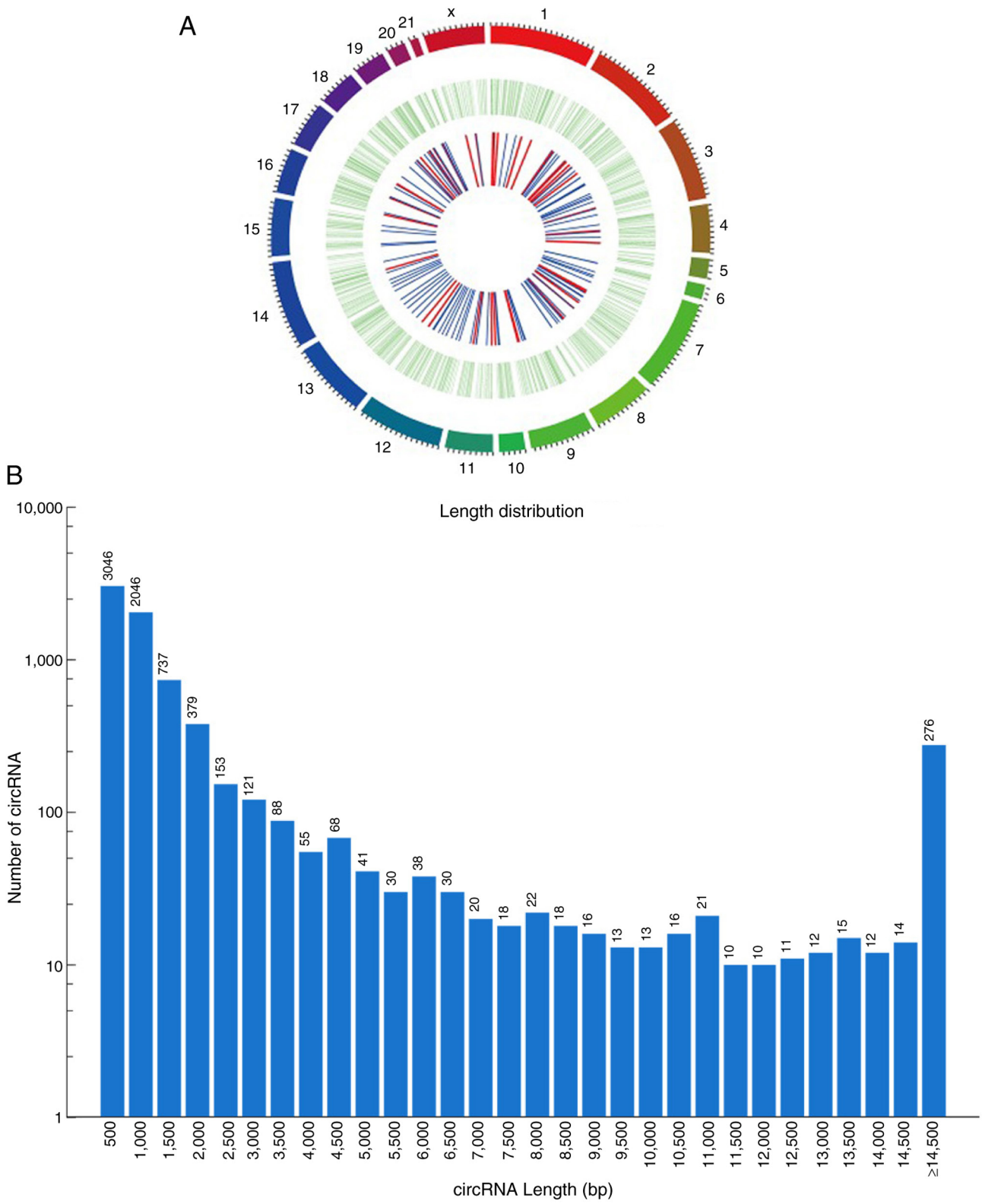

Figure 1. General characteristics of circRNA expression profiles. (A) Circle chart describing the position of circRNA on human chromosomes. Upregulated and downregulated circRNAs are marked with red and blue bars, respectively. Green lines represent the total circRNAs transcripts on chromosomes. (B) Distribution of the sequence length for circRNAs. circRNA, circular RNA.

'GTPase activating protein binding', 'glucocorticoid receptor binding' and various enzyme activities, such as 'transferase activity' and 'phosphotransferase activity, alcohol group as acceptor' (Fig. 3A). The KEGG pathway analysis of these genes was primarily enriched in 'pyruvate metabolism', 'ABC transporters', 'intestinal immune network for IgA production', 'viral myocarditis', 'leishmaniasis', '*Staphylococcus aureus* infection', 'hematopoietic cell lineage', 'toxoplasmosis', 'cell adhesion molecules', 'systemic lupus erythematosus' and 'phagosome' (Fig. 3B).

Table I. DECs between biliary atresia choledochal cyst tissues (16 upregulated and 62 downregulated circRNAs).

Type of DECs	circRNAs
Upregulated	hsa_circ_0006137, hsa_circ_0079422, hsa_circ_0007375, hsa_circ_0005597, hsa_circ_0006961, hsa_circ_0004305, hsa_circ_0002775, hsa_circ_0009096, hsa_circ_0085616, hsa_circ_0026229, hsa_circ_0005654, hsa_circ_0004692, hsa_circ_0023936, hsa_circ_0004383, hsa_circ_0002822, hsa_circ_0008777
Downregulated	hsa_circ_0081171, hsa_circ_0084665, hsa_circ_0075828, hsa_circ_0000374, hsa_circ_0006460, hsa_circ_0005934, hsa_circ_0001747, hsa_circ_0054345, hsa_circ_0067991, hsa_circ_0005047, hsa_circ_0008177, hsa_circ_0003526, hsa_circ_0056744, hsa_circ_0008523, hsa_circ_0002338, hsa_circ_0088088, hsa_circ_0008932, hsa_circ_0001383, hsa_circ_0002485, hsa_circ_0055019, hsa_circ_0061286, hsa_circ_0003113, hsa_circ_0000690, hsa_circ_0004173, hsa_circ_0070942, hsa_circ_0006355, hsa_circ_0054618, hsa_circ_0082002, hsa_circ_0008585, hsa_circ_0008366, hsa_circ_0017160, hsa_circ_0067323, hsa_circ_0005406, hsa_circ_0007518, hsa_circ_0003639, hsa_circ_0032125, hsa_circ_0082415, hsa_circ_0027969, hsa_circ_0008006, hsa_circ_0078299, hsa_circ_0004670, hsa_circ_0004960, hsa_circ_0009069, hsa_circ_0075748, hsa_circ_0020522, hsa_circ_0007262, hsa_circ_0006365, hsa_circ_0019607, hsa_circ_0002220, hsa_circ_0006127, hsa_circ_0001376, hsa_circ_0067480, hsa_circ_0072697, hsa_circ_0084188, hsa_circ_0003456, hsa_circ_0000842, hsa_circ_0001979, hsa_circ_0001771, hsa_circ_0004276, hsa_circ_0014624, hsa_circ_0004179, hsa_circ_0077495

circRNA, circular RNA; DECs, differentially expressed circRNAs.

Validation of DECs using RT-qPCR. Liver tissue samples from 38 patients in the BA group and 54 patients in the CC group were analyzed using RT-qPCR. A total of five significantly upregulated circRNAs (hsa_circ_0006137, hsa_circ_0079422, hsa_circ_0007375, hsa_circ_0005597 and hsa_circ_0006961) and three significantly downregulated circRNAs (hsa_circ_0081171, hsa_circ_0084665 and hsa_circ_0075828) from the R software analysis were selected for RT-qPCR to verify the expression of these DECs. The RT-qPCR results demonstrated that the expression levels of hsa_circ_0006137, hsa_circ_0079422 and hsa_circ_0007375 were significantly increased (Fig. 4A-C), while the expression levels of hsa_circ_0081171 and hsa_circ_0084665 were significantly reduced (Fig. 4F and G) in patients with BA compared with the CC group. However, there was no significant difference in the expression levels of hsa_circ_0005597 and hsa_circ_0006961 between the two groups (Fig. 4D and E). Hsa_circ_0075828 also exhibited a significant increase in patients with BA compared with the CC group (Fig. 4H), contrary to the previous screening results. Therefore, five validated DECs were used for bioinformatics analysis.

Construction of the circRNA regulatory network. An increasing number of studies have demonstrated that circRNAs can increase the expression levels of downstream genes by binding to miRNAs as molecular sponges (32,33). Therefore, 244 potential target miRNAs of hsa_circ_0006137, hsa_circ_0079422, hsa_circ_0007375, hsa_circ_0081171 and hsa_circ_0084665 were predicted through starBase (v2.0). According to competitive endogenous RNA (ceRNA) theory, there is a negative correlation between a circRNA and its target miRNAs (34). Therefore, through a literature search, seven miRNAs were selected as the target miRNAs of the circRNAs (hsa_circ_0006137/miR-26a-5p, hsa_circ_0006137/miR-145-5p, hsa_circ_0079422/miR-593-3p, hsa_circ_0007375/miR-1206, hsa_circ_0007375/miR-1208, hsa_circ_0081171/miR-18a-5p and hsa_circ_0084665/miR-22-5p) for further analysis. Subsequently, 430 target mRNAs were predicted to correspond to these seven miRNAs through the miRDB, miRTarBase and TargetScan databases (Fig. 5A).

Functional analysis of mRNAs. To examine the potential functional role of the five circRNAs, GO and KEGG pathway enrichment analysis on the target mRNAs was carried out. As presented in Fig. 5B, these genes were significantly enriched in the forward transcriptional regulation of 'protein serine/threonine kinase activity', 'RNA polymerase II promoter', 'DNA-binding transcription activator activity, RNA polymerase II-specific', 'DNA-binding transcription factor binding' and 'SMAD binding'. The associated pathways obtained using KEGG analysis were fewer, but 'TGF-β signaling pathway' and 'EGFR tyrosine kinase inhibitor resistance' were included in the enriched pathways (Fig. 5C). In summary, these functional analysis results suggested that the circRNA network may regulate the development of BA through the TGF-β and EGFR signaling pathways, which supports previous study results.

Evaluation of DECs using ROC analysis. To further investigate the diagnostic potential of the aforementioned circRNAs, ROC analysis was used to evaluate the detection sensitivity and specificity. As presented in Fig. 6A-E, the AUC of hsa_circ_0006137, hsa_circ_0079422, hsa_circ_0007375, hsa_circ_0081171 and hsa_circ_0084665 in the differential diagnosis of BA compared with CC was >0.8, indicating that

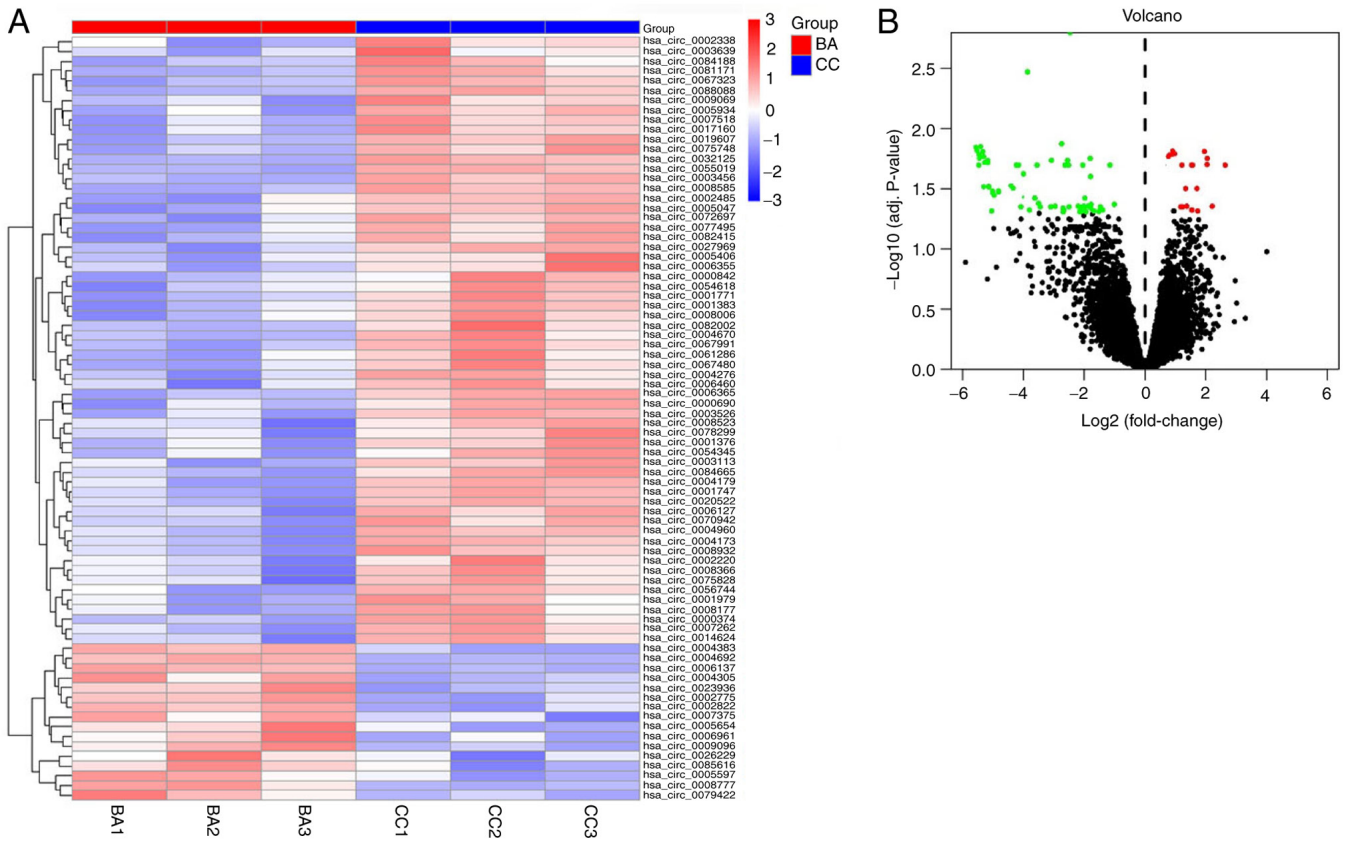

Figure 2. Heatmap and volcano plot of DECs. (A) Heatmap indicating 16 upregulated circRNAs and 62 downregulated circRNAs; different rows represent the different genes. Red, upregulated genes; blue, downregulated genes. (B) Volcano plot representing circRNA expression in BA. Black points, normally expressed circRNAs; red points, upregulated DECs; and green points, downregulated DECs. BA, biliary atresia; CC, choledochal cyst; circRNA, circular RNA; DECs, differentially expressed circRNAs; adj., adjusted.

these circRNAs have a relatively high sensitivity and specificity for BA. These findings suggested that these circRNAs may serve as potential indicators for distinguishing BA from CC and could offer important insights for clinical research.

Discussion

BA is a destructive inflammatory disease, Lakshminaraya nan and Davenport (35) demonstrated that viral infection, toxicological effects and gene mutations may be associated with it. In previous years, research has been devoted to investigating new therapeutic targets and biomarkers of BA. For example, Girard and Panasyuk (36) revealed an abnormal expression of a number of genes (such as GPC1 and TCF4) in BA. High-throughput sequencing technology has broadened the understanding of gene regulatory networks. Genome-wide sequencing demonstrated that ~93% of the genome is transcribed into RNA, but only 2% encodes proteins (37). Although the total number of nucleotides in the human genome is 30 times that of the nematode genome, the number of protein coding sequences is similar, which highlights the importance of non-coding RNA (ncRNA) sequences in regulating eukaryotic gene expression (38). With the widespread acceptance of the concept of ceRNA suggested by Salmena *et al* (39), miRNA has become the core of the ncRNA regulatory network. Calvopina *et al* (40) revealed that numerous types of miRNAs are specifically expressed in the tissues of children with BA, which proves that the gene regulatory network centered on miRNA may serve an important role in the pathogenesis of BA. Previously, circRNA has been revealed to serve as an important ceRNA that can regulate gene expression at the posttranscriptional level by binding to target miRNAs (41). Due to further research, an increasing number of circRNAs have been revealed to be new diagnostic markers for diseases, including cancer (42,43). However, there have only been a small number of reports on circRNAs associated with BA.

To the best of our knowledge, the present study is the first to analyze the circRNA regulatory network of BA, revealing 16 upregulated circRNAs and 62 downregulated circRNAs. The function of the DECs was investigated using GO and KEGG enrichment analysis. In addition, three upregulated circRNAs and two downregulated circRNAs were verified using RT-qPCR. GO enrichment analysis of the DECs indicated that 'regulation of catabolic process', 'regulation of cellular catabolic process' and 'positive regulation of biological process' were mostly enriched in the biological process category, indicating that the disturbance of energy metabolism may promote the occurrence of BA. In terms of cell component and molecular function, the membrane region and transferase activity indict that intercellular junction and the enrichment of extracellular matrix were involved, which may be associated with the damage of bile duct epithelial cells and the inflammatory infiltration of the bile duct in BA. KEGG analysis

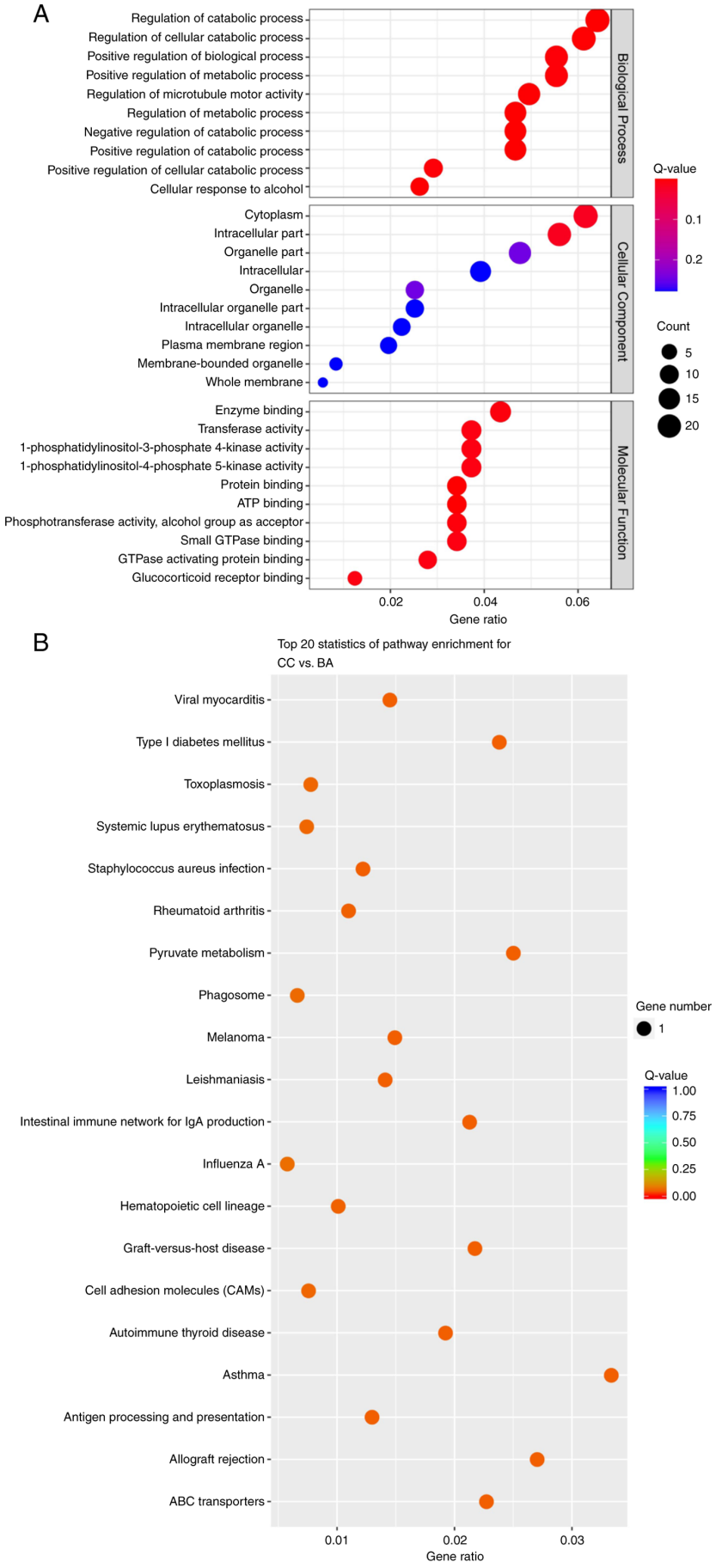

Figure 3. GO and KEGG pathway analysis of DECs identified using R software. (A) GO terms of the biological process, cell component and molecular function enrichment category of the 78 DECs. (B) KEGG pathway analysis of the 78 DECs. DECs, differentially expressed circular RNAs; BA, biliary atresia; CC, choledochal cyst; GO, Gene Ontology; KEGG, Kyoto Encyclopedia of Genes and Genomes.

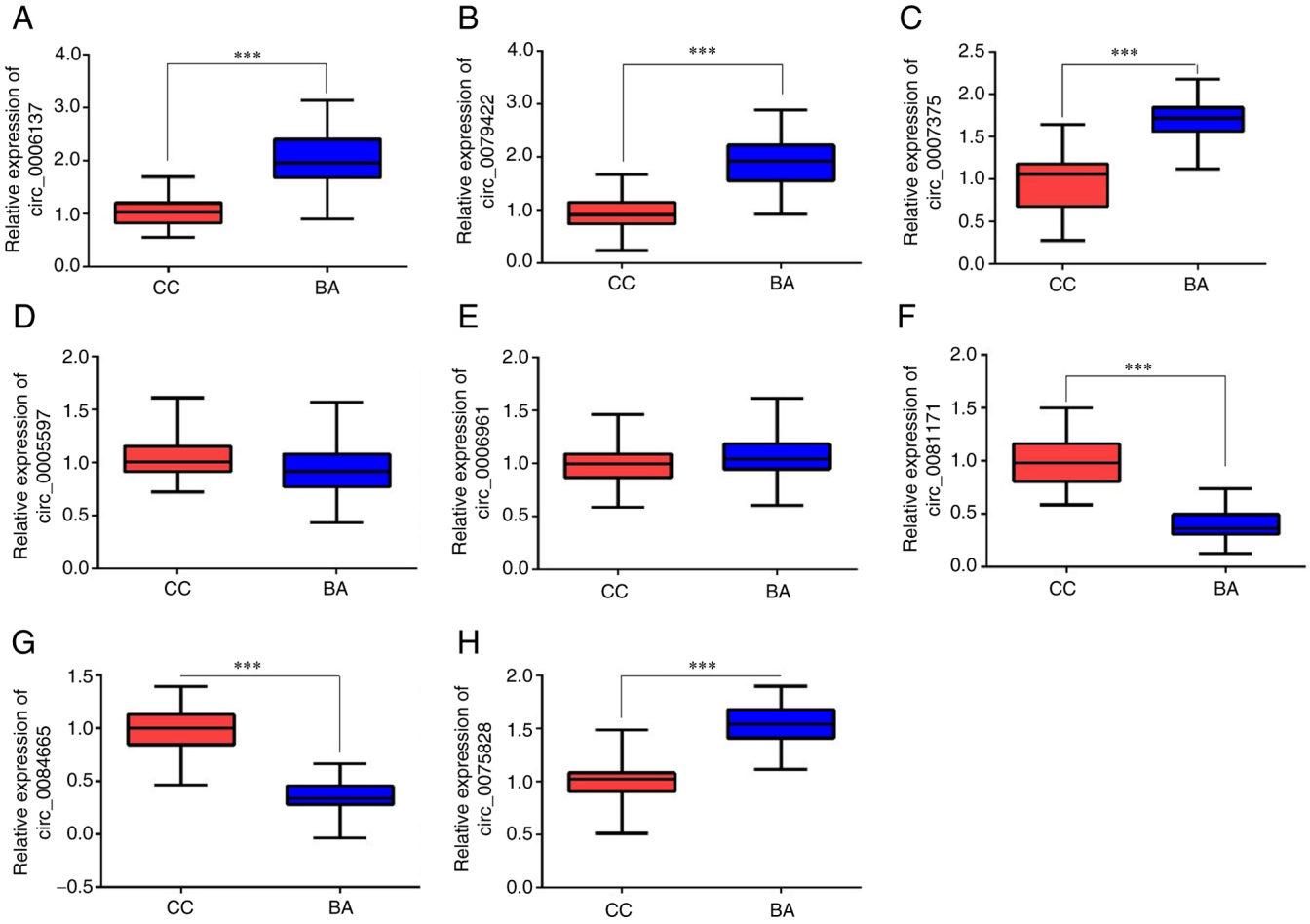

Figure 4. Validation of eight DECs using reverse transcription-quantitative polymerase chain reaction. A total of three circRNAs, including (A) hsa_circ_0006137, (B) hsa_circ_0079422 and (C) hsa_circ_0007375, were significantly upregulated in BA liver tissues compared with CC tissues. The levels of (D) hsa_circ_0005597 and (E) hsa_circ_0006961 were not significantly different between BA and CC tissues. A total of two circRNAs, including (F) hsa_circ_0081171 and (G) hsa_circ_0084665, were significantly downregulated in BA liver tissues compared with CC tissues. (H) Hsa_circ_0075828 demonstrated an upregulation trend in BA. ***P<0.001. BA, biliary atresia; CC, choledochal cyst; circRNA, circular RNA.

demonstrated that 'myocarditis' was significantly enriched. A previous study demonstrated that bacteremia caused by golden *Staphylococci* can be complicated with endocarditis, metastatic infection or septicemia syndrome (44). Furthermore, patients with liver disease can experience lesions of the biliary tract or gallbladder (45,46).

In the present study, three upregulated circRNAs were identified to bind to five miRNAs. According to previous studies, miR-26a-5p can increase the transcriptional level of THAP domain-containing protein 2 and induce apoptosis in endometrial cancer cells (47). In a mouse model of myocardial infarction, the expression of miR-26a-5p was downregulated in myocardial cells following ischemia-reperfusion injury, and myocardial ischemia-reperfusion injury was regulated by the expression level of PTEN gene through the PI3K/AKT signaling pathway (48). In our previous study, it was revealed that the expression level of miR-145 was significantly decreased in BA (49), while in the present study, it was revealed that the upregulated hsa_circ_0006137 had a binding site for miR-145, which may be the reason for the downregulation of the latter in BA. In osteosarcoma, miR-593-3p can inhibit tumorigenesis by promoting the upregulation of zinc finger E-box binding homeobox 2 (50). SNHG14 (51) and MAP3K2 (52) genes have been shown to serve as targets of miR-1206 and miR-1208 respectively, and miR-1206 and miR-1208 can act as targets for tumor suppression.

To fully understand the effects of circRNA-associated regulatory networks on BA, the miRNA-circRNA and miRNA-mRNA interaction was predicted. GO and KEGG enrichment analyses of the genes in this network were carried out and revealed that the enrichment terms were associated with the pathogenesis of BA. GO enrichment analysis suggested that these mRNAs were involved in the 'DNA-binding transcription activator activity, RNA polymerase II-specific'. The results of the KEGG pathway enrichment analysis demonstrated that these downstream target genes were significantly enriched in the 'TGF-β signaling pathway', while enrichment of 'EGFR tyrosine kinase inhibitor resistance' was also observed. The EGFR family is one of the most studied receptor protein tyrosine kinases, because it serves a universal role in signal transduction and tumorigenesis (53). Activation of the TGF-β signaling pathway can increase the expression levels of extracellular matrix proteins (such as SMAD and PI3K) (54), cause an imbalance between extracellular matrix production and degradation, and promote the occurrence of

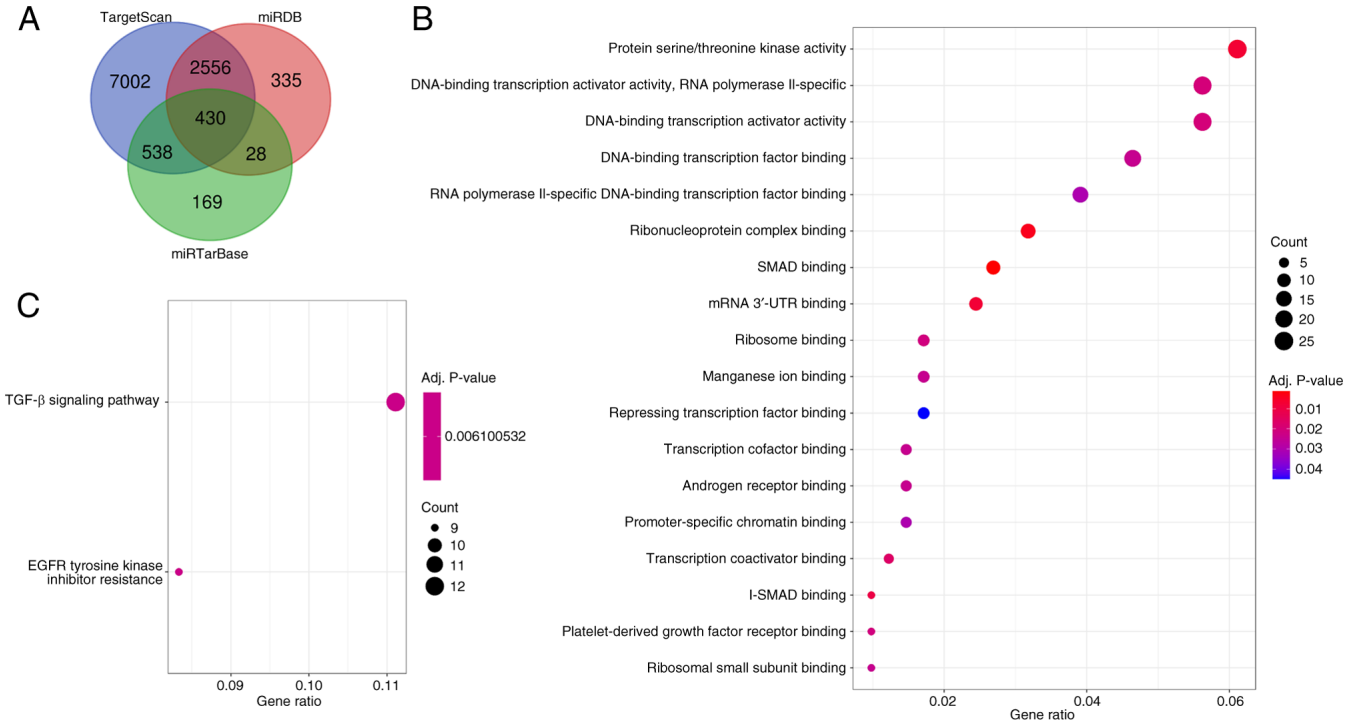

Figure 5. Functional analysis of mRNAs. Using three databases, seven microRNAs were predicted and then intersected to obtain 430 target mRNAs. (A) Venn diagram of predicted target mRNAs (B) Gene Ontology analysis and (C) Kyoto Encyclopedia of Genes and Genomes pathway analysis of the 430 target mRNAs. UTR, untranslated region.

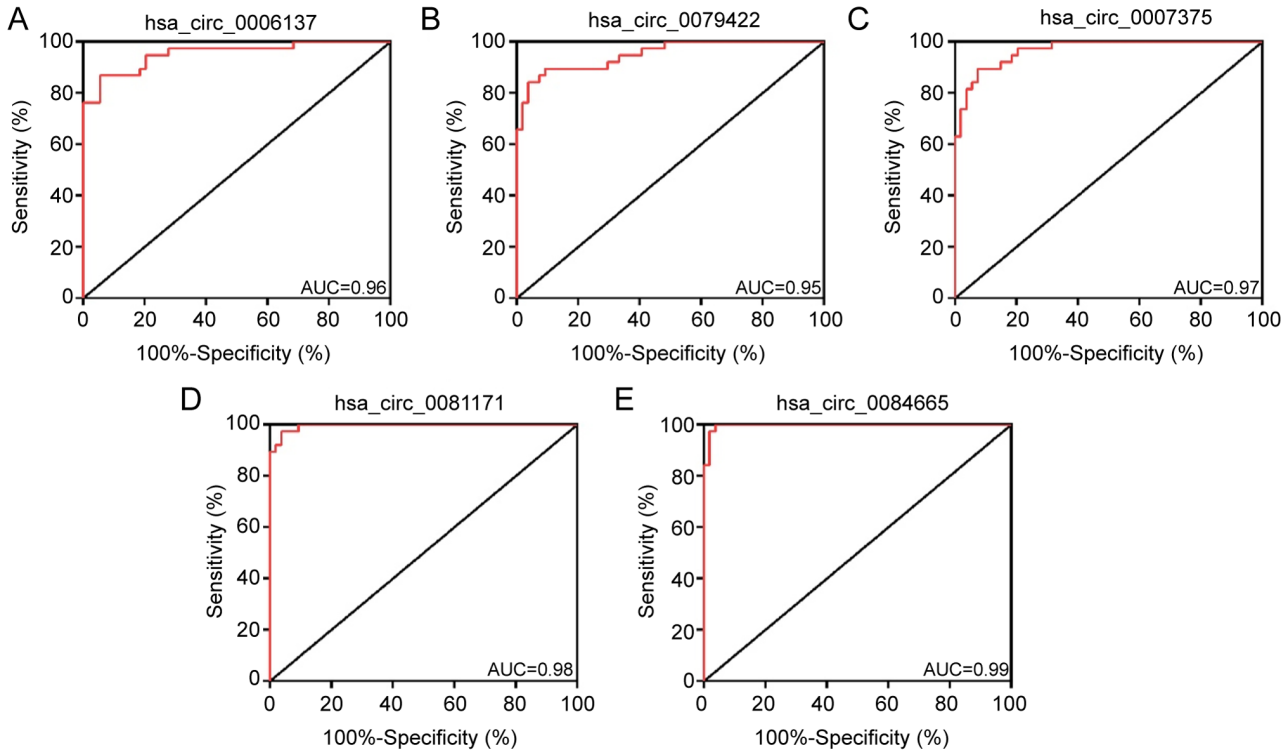

Figure 6. ROC curve analysis. ROC curve analysis revealed the sensitivity and specificity of (A) hsa_circ_0006137, (B) hsa_circ_0079422, (C) hsa_circ_0007375, (D) hsa_circ_0081171 and (E) hsa_circ_0084665 in patients with biliary atresia. ROC, receiver operating characteristic; AUC, area under the curve.

BA. For example, Chung-Davidson *et al* (55) revealed that BA cholangiopathy can be delayed by blocking the TGF-β signaling pathway.

Therefore, the present study suggests that the identified DECs may be associated with BA by regulating gene expression. Further investigations should be performed by

experimental methods such as dual-luciferase activity experiment and PCR tests. Further verification of the interaction of circRNAs with miRNAs and in-depth study of the function of circRNAs and their effect on cell regulation should be performed. While the present study revealed important insights into the circRNA regulatory network of BA, it should acknowledge certain limitations. One such limitation was the use of the same samples for both identification and validation of circRNAs. Using the same samples for both stages of the study can introduce bias, as the validation stage was not independent of the identification stage. However, the findings of the present study offered a foundation for future research, and further studies with independent validation cohorts to validate and expand upon the present results should be performed.

In conclusion, the present study obtained a circRNA map of BA liver tissue based on RNA high-throughput sequencing and identified 78 DECs. Subsequently, the expression of three upregulated circRNAs and two downregulated circRNAs in BA liver tissues were further verified. Moreover, circRNA regulatory networks in BA were constructed for the first time and their potential biological functions were analyzed. The study of the circRNA-miRNA pathway may provide further insights for examining the pathogenesis of BA. Thus, the potential molecular mechanism of circRNAs in BA require further elucidation. However, it is important to note that these results were not directly associated with prognosis, as no clinical data were considered in the present analysis. Future studies should incorporate relevant clinical data to evaluate the prognostic potential of these circRNAs.

Acknowledgements

Not applicable.

Funding

The present study was supported by the Shenzhen Medical and Health Project (grant no. SZSM201812055), the National Natural Science Foundation of China (grant no. 81770512) and the Medical Science and Technology Research Foundation of Guangdong Province (grant no. A2019541).

Availability of data and materials

The sequencing datasets generated and/or analyzed during the current study are available in Gene Expression Omnibus (https://www.ncbi.nlm.nih.gov/geo/query/acc.cgi?acc=GSE240795). All other datasets used and/or analyzed during the current study are available from the corresponding author on reasonable request.

Authors' contributions

DL and YD designed the study. DL, YD and JG conducted the experiments. ZW, LZ and BW analyzed the data and wrote the manuscript. All authors read and approved the final version of the manuscript. DL, YD, JG, ZW, LZ and BW confirm the authenticity of all the raw data.

Ethics approval and consent to participate

All procedures performed in studies involving human participants were approved by the Ethics Committee of Shenzhen Children's Hospital (Shenzhen, China; approval no. SUMC2017-026). The parents/guardians of all subjects signed a written informed consent form.

Patient consent for publication

Not applicable.

Competing interests

The authors declare that they have no competing interests.

References

1. Kawano Y, Yoshimaru K, Uchida Y, Kajihara K, Toriigahara Y, Shirai T, Takahashi Y and Matsuura T: Biliary atresia in a preterm and extremely low birth weight infant: A case report and literature review. Surg Case Rep 6: 321, 2020.
2. Bezerra JA, Wells RG, Mack CL, Karpen SJ, Hoofnagle JH, Doo E and Sokol RJ: Biliary atresia: Clinical and research challenges for the twenty-first century. Hepatology 68: 1163-1173, 2018.
3. Hsiao CH, Chang MH, Chen HL, Lee HC, Wu TC, Lin CC, Yang YJ, Chen AC, Tiao MM, Lau BH, *et al*: Universal screening for biliary atresia using an infant stool color card in Taiwan. Hepatology 47: 1233-1240, 2008.
4. Hartley JL, Davenport M and Kelly DA: Biliary atresia. Lancet 374: 1704-1713, 2009.
5. Davenport M, Tizzard SA, Underhill J, Mieli-Vergani G, Portmann B and Hadzić N: The biliary atresia splenic malformation syndrome: A 28-year single-center retrospective study. J Pediatr 149: 393-400, 2006.
6. Hartley JL, O'Callaghan C, Rossetti S, Consugar M, Ward CJ, Kelly DA and Harris PC: Investigation of primary cilia in the pathogenesis of biliary atresia. J Pediatr Gastroenterol Nutr 52: 485-488, 2011.
7. Fabris L, Cadamuro M, Guido M, Spirli C, Fiorotto R, Colledan M, Torre G, Alberti D, Sonzogni A, Okolicsanyi L and Strazzabosco M: Analysis of liver repair mechanisms in Alagille syndrome and biliary atresia reveals a role for notch signaling. Am J Pathol 171: 641-653, 2007.
8. Muraji T: Biliary atresia: New lessons learned from the past. J Pediatr Gastroenterol Nutr 53: 586-587, 2011.
9. Edom PT, Meurer L, da Silveira TR, Matte U and dos Santos JL: Immunolocalization of VEGF A and its receptors, VEGFR1 and VEGFR2, in the liver from patients with biliary atresia. Appl Immunohistochem Mol Morphol 19: 360-368, 2011.
10. Bolha L, Ravnik-Glavač M and Glavač D: Circular RNAs: Biogenesis, function, and a role as possible cancer biomarkers. Int J Genomics 2017: 6218353, 2017.
11. Zeng X, Lin W, Guo M and Zou Q: A comprehensive overview and evaluation of circular RNA detection tools. PLoS Comput Biol 13: e1005420, 2017.
12. Verduci L, Strano S, Yarden Y and Blandino G: The circRNA-microRNA code: Emerging implications for cancer diagnosis and treatment. Mol Oncol 13: 669-680, 2019.
13. Hansen TB, Wiklund ED, Bramsen JB, Villadsen SB, Statham AL, Clark SJ and Kjems J: miRNA-dependent gene silencing involving Ago2-mediated cleavage of a circular antisense RNA. EMBO J 30: 4414-4422, 2011.
14. Abdelmohsen K, Panda AC, Munk R, Grammatikakis I, Dudekula DB, De S, Kim J, Noh JH, Kim KM, Martindale JL and Gorospe M: Identification of HuR target circular RNAs uncovers suppression of PABPN1 translation by CircPABPN1. RNA Biol 14: 361-369, 2017.
15. Miao Q, Zhong Z, Jiang Z, Lin Y, Ni B, Yang W and Tang J: RNA-seq of circular RNAs identified circPTPN22 as a potential new activity indicator in systemic lupus erythematosus. Lupus 28: 520-528, 2019.

16. Li LJ, Zhu ZW, Zhao W, Tao SS, Li BZ, Xu SZ, Wang JB, Zhang MY, Wu J, Leng RX, *et al*: Circular RNA expression profile and potential function of hsa_circ_0045272 in systemic lupus erythematosus. Immunology 155: 137-149, 2018.
17. Wang L, Shen C, Wang Y, Zou T, Zhu H, Lu X, Li L, Yang B, Chen J, Chen S, *et al*: Identification of circular RNA Hsa_circ_0001879 and Hsa_circ_0004104 as novel biomarkers for coronary artery disease. Atherosclerosis 286: 88-96, 2019.
18. Lei M, Zheng G, Ning Q, Zheng J and Dong D: Translation and functional roles of circular RNAs in human cancer. Mol Cancer 19: 30, 2020.
19. Floris G, Zhang L, Follesa P and Sun T: Regulatory role of circular RNAs and neurological disorders. Mol Neurobiol 54: 5156-5165, 2017.
20. Zhang X, Lu N, Wang L, Wang Y, Li M, Zhou Y, Yan H, Cui M, Zhang M and Zhang L: Circular RNAs and esophageal cancer. Cancer Cell Int 20: 362, 2020.
21. Chen X, Zhu S, Li HD, Wang JN, Sun LJ, Xu JJ, Hui YR, Li XF, Li LY, Zhao YX, *et al*: N^6-methyladenosine-modified circIRF2, identified by YTHDF2, suppresses liver fibrosis via facilitating FOXO3 nuclear translocation. Int J Biol Macromol 248: 125811, 2023.
22. Wang Q, Long Z, Zhu F, Li H, Xiang Z, Liang H, Wu Y, Dai X and Zhu Z: Integrated analysis of lncRNA/circRNA-miRNA-mRNA in the proliferative phase of liver regeneration in mice with liver fibrosis. BMC Genomics 24: 417, 2023.
23. Bolger AM, Lohse M and Usadel B: Trimmomatic: A flexible trimmer for Illumina sequence data. Bioinformatics 30: 2114-2120, 2014.
24. Kozomara A and Griffiths-Jones S: miRBase: Annotating high confidence microRNAs using deep sequencing data. Nucleic Acids Res 42 (Database Issue): D68-D73, 2014.
25. Friedländer MR, Mackowiak SD, Li N, Chen W and Rajewsky N: miRDeep2 accurately identifies known and hundreds of novel microRNA genes in seven animal clades. Nucleic Acids Res 40: 37-52, 2012.
26. Robinson MD, McCarthy DJ and Smyth GK: edgeR: A Bioconductor package for differential expression analysis of digital gene expression data. Bioinformatics 26: 139-140, 2010.
27. Livak KJ and Schmittgen TD: Analysis of relative gene expression data using real-time quantitative PCR and the 2(-Delta Delta C(T)) method. Methods 25: 402-408, 2001.
28. Li JH, Liu S, Zhou H, Qu LH and Yang JH: starBase v2.0: Decoding miRNA-ceRNA, miRNA-ncRNA and protein-RNA interaction networks from large-scale CLIP-Seq data. Nucleic Acids Res 42 (Database Issue): D92-D97, 2014.
29. Szklarczyk D, Gable AL, Lyon D, Junge A, Wyder S, Huerta-Cepas J, Simonovic M, Doncheva NT, Morris JH, Bork P, *et al*: STRING v11: Protein-protein association networks with increased coverage, supporting functional discovery in genome-wide experimental datasets. Nucleic Acids Res 47 (D1): D607-D613, 2019.
30. Shannon P, Markiel A, Ozier O, Baliga NS, Wang JT, Ramage D, Amin N, Schwikowski B and Ideker T: Cytoscape: A software environment for integrated models of biomolecular interaction networks. Genome Res 13: 2498-2504, 2003.
31. Robin X, Turck N, Hainard A, Tiberti N, Lisacek F, Sanchez JC and Müller M: pROC: An open-source package for R and S+ to analyze and compare ROC curves. BMC Bioinformatics 12: 77, 2011.
32. Xu X, Song B, Zhang Q, Qi W and Xu Y: Hsa_circ_0022383 promote non-small cell lung cancer tumorigenesis through regulating the miR-495-3p/KPNA2 axis. Cancer Cell Int 23: 282, 2023.
33. Zhang C and He W: Circ_0020014 mediates CTSB expression and participates in IL-1β-prompted chondrocyte injury via interacting with miR-24-3p. J Orthop Surg Res 18: 877, 2023.
34. Karreth FA, Reschke M, Ruocco A, Ng C, Chapuy B, Léopold V, Sjoberg M, Keane TM, Verma A, Ala U, *et al*: The BRAF pseudogene functions as a competitive endogenous RNA and induces lymphoma in vivo. Cell 161: 319-332, 2015.
35. Lakshminarayanan B and Davenport M: Biliary atresia: A comprehensive review. J Autoimmun 73: 1-9, 2016.
36. Girard M and Panasyuk G: Genetics in biliary atresia. Curr Opin Gastroenterol 35: 73-81, 2019.
37. Debray D, Corvol H and Housset C: Modifier genes in cystic fibrosis-related liver disease. Curr Opin Gastroenterol 35: 88-92, 2019.
38. Costa FF: Non-coding RNAs, epigenetics and complexity. Gene 410: 9-17, 2008.
39. Salmena L, Poliseno L, Tay Y, Kats L and Pandolfi PP: A ceRNA hypothesis: The Rosetta Stone of a hidden RNA language? Cell 146: 353-358, 2011.
40. Calvopina DA, Coleman MA, Lewindon PJ and Ramm GA: Function and regulation of microRNAs and their potential as biomarkers in paediatric liver disease. Int J Mol Sci 17: 1795, 2016.
41. Vicens Q and Westhof E: Biogenesis of circular RNAs. Cell 159: 13-14, 2014.
42. Li H, Zheng X, Gao J, Leung KS, Wong MH, Yang S, Liu Y, Dong M, Bai H, Ye X and Cheng L: Whole transcriptome analysis reveals non-coding RNA's competing endogenous gene pairs as novel form of motifs in serous ovarian cancer. Comput Biol Med 148: 105881, 2022.
43. Wu S, Wu Y, Deng S, Lei X and Yang X: Emerging roles of noncoding RNAs in human cancers. Discov Oncol 14: 128, 2023.
44. Ramljak S, Schmitz M, Repond C, Zerr I and Pellerin L: Altered mRNA and protein expression of monocarboxylate transporter MCT1 in the cerebral cortex and cerebellum of prion protein knockout mice. Int J Mol Sci 22: 1566, 2021.
45. Acalovschi M: Gallstones in patients with liver cirrhosis: Incidence, etiology, clinical and therapeutical aspects. World J Gastroenterol 20: 7277-7285, 2014.
46. Konyn P, Alshuwaykh O, Dennis BB, Cholankeril G, Ahmed A and Kim D: Gallstone disease and its association with nonalcoholic fatty liver disease, all-cause and cause-specific mortality. Clin Gastroenterol Hepatol 21: 940-948.e2, 2023.
47. Li M, Xiao Y, Liu M, Ning Q, Xiang Z, Zheng X, Tang S and Mo Z: MiR-26a-5p regulates proliferation, apoptosis, migration and invasion via inhibiting hydroxysteroid dehydrogenase like-2 in cervical cancer cell. BMC Cancer 22: 876, 2022.
48. Xing X, Guo S, Zhang G, Liu Y, Bi S, Wang X and Lu Q: miR-26a-5p protects against myocardial ischemia/reperfusion injury by regulating the PTEN/PI3K/AKT signaling pathway. Braz J Med Biol Res 53: e9106, 2020.
49. Ye Y, Li Z, Feng Q, Chen Z, Wu Z, Wang J, Ye X, Zhang D, Liu L, Gao W, *et al*: Downregulation of microRNA-145 may contribute to liver fibrosis in biliary atresia by targeting ADD3. PLoS One 12: e0180896, 2017.
50. Zhang C, Zhou H, Yuan K, Xie R and Chen C: Overexpression of hsa_circ_0136666 predicts poor prognosis and initiates osteosarcoma tumorigenesis through miR-593-3p/ZEB2 pathway. Aging (Albany NY) 12: 10488-10496, 2020.
51. Abd El-Aziz A, El-Desouky MA, Shafei A, Elnakib M and Abdelmoniem AM: Influence of pentoxifylline on gene expression of PAG1/miR-1206/SNHG14 in ischemic heart disease. Biochem Biophys Rep 25: 100911, 2021.
52. Zhang Y, Wang D, Zhu T, Yu J, Wu X, Lin W, Zhu M, Dai Y and Zhu J: CircPUM1 promotes hepatocellular carcinoma progression through the miR-1208/MAP3K2 axis. J Cell Mol Med 25: 600-612, 2021.
53. Roskoski R Jr: Small molecule inhibitors targeting the EGFR/ErbB family of protein-tyrosine kinases in human cancers. Pharmacol Res 139: 395-411, 2019.
54. Tzavlaki K and Moustakas A: TGF-β signaling. Biomolecules 10: 487, 2020.
55. Chung-Davidson YW, Ren J, Yeh CY, Bussy U, Huerta B, Davidson PJ, Whyard S and Li W: TGF-β signaling plays a pivotal role during developmental biliary atresia in sea lamprey (petromyzon marinus). Hepatol Commun 4: 219-234, 2019.